Trimethylguanosine Synthase1 (TGS1) Is Essential for Chilling Tolerance[1][OPEN]

Jinpeng Gao, James G. Wallis, Jeremy B. Jewell, and John Browse[2]

Institute of Biological Chemistry, Clark Hall, Washington State University, Pullman, Washington 99164-6340

ORCID IDs: 0000-0002-9249-1067 (J.G.); 0000-0002-2554-2821 (J.B.).

Chilling stress is a major factor limiting plant development and crop productivity. Because the plant response to chilling is so complex, we are far from understanding the genes important in the response to chilling. To identify new genes important in chilling tolerance, we conducted a novel mutant screen, combining a confirmed SALK T-DNA insertion collection with traditional forward genetics. We screened a pool of more than 3700 confirmed homozygous SALK T-DNA insertion lines for visible defects under prolonged growth at 5°C. Of the chilling-sensitive mutants we observed, mutations at one locus were characterized in detail. This gene, At1g45231, encodes an Arabidopsis (*Arabidopsis thaliana*) trimethylguanosine synthase (TGS1), previously uncharacterized in the plant kingdom. We confirmed that Arabidopsis TGS1 is a functional ortholog of other trimethylguanosine synthases based both on its in vitro methyltransferase activity and on its ability to rescue the cold-growth inhibition of a *Saccharomyces cerevisiae tgs1Δ* mutant in vivo. While *tgs1* mutant plants grew normally at 22°C, their vegetative and reproductive growth was severely compromised under chilling conditions. When we transgenically expressed *TGS1* in the mutant plants, the chilling-sensitive phenotype was relieved, demonstrating that TGS1 is required for chilling tolerance.

Low temperature is a critical environmental stress for many plants. Cold reduces seed germination, inhibits vegetative growth, lowers reproductive success, slows seed and fruit development, and even threatens survival; it also limits the geographical distribution of plants (Levitt, 1980; Wang, 1990; Zinn et al., 2010; Barrero-Gil et al., 2016). Plant species originating in temperate regions accommodate to cold and survive even when exposed to prolonged freezing temperature (Thomashow, 1999). In contrast to such chilling-tolerant species, more than half of plant species on earth have origins in tropical regions, and many of these chilling-sensitive plants may be seriously damaged or killed when exposed to low, nonfreezing temperatures. The chilling damage that occurs between 0°C and 15°C is sometimes subtle, and distinct from freezing damage that occurs when temperatures fall below 0°C. Chilling-sensitive plants undergo a range of physiological changes when exposed to low temperatures, including increased electrolyte leakage through the plasma membrane and decreased photosynthetic capacity (Lyons, 1973; Allen and Ort, 2001). The diverse external symptoms of plant chilling injury include cessation of growth, wilting, chlorosis, necrosis, and eventual death.

The economic importance of chilling injury to world agriculture has been recognized for more than 100 years because chilling has a large impact on crops. Many significant crops have their origins in tropical regions and are chilling sensitive, including rice (*Oryza sativa*), maize (*Zea mays*), cucumber (*Cucumis sativus*), cotton (*Gossypium hirsutum*), and soybean (*Glycine max*; Lyons, 1973; Wang, 1990; Ma et al., 2015; Lv et al., 2016). Understanding the mechanisms of chilling sensitivity and improving chilling tolerance of these crops would greatly benefit world food supplies, both by directly reducing crop damage and by expanding arable acreage into colder areas (Wang, 1990; Foyer et al., 2002).

Many studies of chilling sensitivity have focused on the physiological and biological processes contributing to chilling injury, with a view to developing technological methods to ameliorate chilling damage (Lyons, 1973; Wang, 1990; Guan et al., 2009; Lin and Block, 2010; Lukatkin et al., 2012). These investigations are hampered by poor understanding of the complex changes produced under chilling stress, making determination of which specific changes are critical to chilling stress difficult. In fact, plant responses to chilling treatments alter almost all aspects of growth and metabolism (Usadel et al., 2008). Efforts to improve chilling tolerance have included genetic crossing of chilling-sensitive plants with related but chilling-tolerant species, as in tomato (*Solanum lycopersicum*) and orchid (*Sarcochilus hartmannii*) (Vallejos and Pearcy, 1987; Patterson and Reid, 1990). Unfortunately,

[1] This work was supported by grant no. IOS-1555581 from the U.S. National Science Foundation and by the Agricultural Research Center at Washington State University.

[2] Address correspondence to jab@wsu.edu.

The author responsible for distribution of materials integral to the findings presented in this article in accordance with the policy described in the Instructions for Authors (www.plantphysiol.org) is: John Browse (jab@wsu.edu).

J.G. and J.B. conceived the research project; J.G. performed experiments with help of J.B.J.; all authors were involved in writing the manuscript.

[OPEN] Articles can be viewed without a subscription.

www.plantphysiol.org/cgi/doi/10.1104/pp.17.00340

the chilling tolerance of such interbred crops proved unstable in subsequent generations. A new approach based on mutant analysis could overcome the limitations of previous studies by detecting individual determinants of chilling tolerance and sensitivity, with a view to creation of crops with greater resistance to chilling damage.

While chilling-sensitive plants evolved in warm regions without selection pressure to favor low-temperature growth, plants evolving in cooler climates have necessarily developed chilling tolerance mechanisms to thrive in temperate regions. Mutation of such chilling-resistant plants, followed by screening for phenotype defects under chilling conditions, should pinpoint loci that enable chilling tolerance, providing valuable genetic information and identifying the mechanisms of chilling damage. The model plant Arabidopsis (*Arabidopsis thaliana*) is a chilling-resistant plant whose use has drastically accelerated discovery in all fields of plant biology. Arabidopsis is amenable to mutation and screening for phenotypes, and mutant loci are readily identified (Provart et al., 2016). This model plant can therefore be used to identify chilling tolerance mechanisms that may be broadly applicable to the plant kingdom (Porat and Guy, 2007), with the potential of incorporating the findings into horticulturally important chilling-sensitive plants (Tokuhisa, 1999).

Arabidopsis plants mutagenized either by chemical means or by T-DNA insertion have previously been screened for chilling phenotypes and key gene loci revealed. For example, *pfc1* encodes an 18S rRNA demethylase required for chloroplast development at low temperature (Schneider et al., 1995; Tokuhisa et al., 1997, 1998). In addition, mutants in the *fatty acid biosynthesis1* gene suffer collapse of photosynthesis and degradation of chloroplasts when exposed to low temperature for long periods, due to changed membrane lipids (Wu et al., 1997; Gao et al., 2015). The importance of two Arabidopsis chloroplast RNA binding proteins to chilling tolerance through their role in chloroplast RNA processing was revealed by mutant analysis (Kupsch et al., 2012; Wang et al., 2016). While the gene loci so far identified affect either membrane lipid synthesis or chloroplast RNA processing, the complexity of changes induced by chilling suggests that many more loci important to chilling tolerance are yet to be identified.

To discover novel genes important to chilling stress, we chose to exploit a large Arabidopsis genetic resource, the confirmed SALK T-DNA insertion mutant pools. These pools are intended to blanket the entire Arabidopsis genome with one insertion in each gene (Provart et al., 2016). When this mutant resource is combined with traditional forward genetics, time-consuming gene mapping is avoided since the insertion locus for each line has been identified. In addition, because the pools are intended to contain only one insertion for each gene, no locus will be repeatedly identified. We screened more than 3700 confirmed homozygous SALK T-DNA insertion lines under chilling conditions and selected one chilling-sensitive mutant for detailed analysis. The mutant gene (At1g45231) encodes an Arabidopsis trimethylguanosine synthase (TGS1) previously uncharacterized in the plant kingdom. We confirmed that the Arabidopsis TGS1 is a functional ortholog of other trimethylguanosine synthases based both on its in vitro methyltransferase activity and on its ability in vivo to rescue the cold growth inhibition phenotype of a *Saccharomyces cerevisiae tgs1*Δ mutant. While three independent lines with insertions in this locus grew normally at 22°C, both vegetative and reproductive growth of mutants were severely compromised under the chilling conditions. When we expressed *TGS1* as a transgene in these plants, their chilling-sensitive phenotype was relieved, demonstrating that the mutations in *tgs1* caused chilling sensitivity.

RESULTS

Isolation of a Chilling-Sensitive Mutant

A collection of independent, confirmed SALK lines were obtained from the Arabidopsis Biological Resource Center (ABRC); each T-DNA line contains a single insertion whose location has been determined by genomic sequencing (Alonso et al., 2003). All 3739 lines were screened under chilling conditions at 5°C for a period of 8 to 20 weeks; 41 T-DNA lines that exhibited a visible phenotype under these conditions were identified (Supplemental Table S1). When we grew these selected lines at 22°C, 12 of them had visible phenotypes at the warmer temperature that were similar to their cold phenotypes and were not further investigated, since their defect was not specific to the cold. Eight of the remaining mutants were in loci that had already been examined by others. We sought second alleles of the remaining uncharacterized cold-sensitive mutants to confirm that the phenotype was replicated with another lesion in the same locus, but for 13 lines, no second allele was available. For only one of the remaining eight lines did the second allele have a chilling-sensitive phenotype like the allele detected in the primary screen (Supplemental Table S1), so we chose to examine in detail the lines mutant at this locus.

The plant line detected in the screen carried the *SALK_084665* insertion and exhibited a very strong visible phenotype when grown at 5°C but grew normally at 22°C. The insertion in *SALK_084665* was characterized as interrupting the last of 12 exons in At1g45231 (Fig. 1). The second allele we obtained, *SALK_071651*, was annotated as interrupting the same open reading frame in exon eight. When tested, *SALK_071651* exhibited the same chilling phenotype as *SALK_084665* and also grew normally at 22°C. We later identified and characterized a third allele, *SALK_020980*, an insertion in the fifth exon of the same gene (Fig. 1), whose phenotype was indistinguishable from the first two alleles. We examined expression of At1G45231 in the insertion lines using primers designed to amplify the full-length open reading frame, using cDNA reverse-transcribed from RNA isolated from each mutant line and from wild type control plants. Amplification from the wild

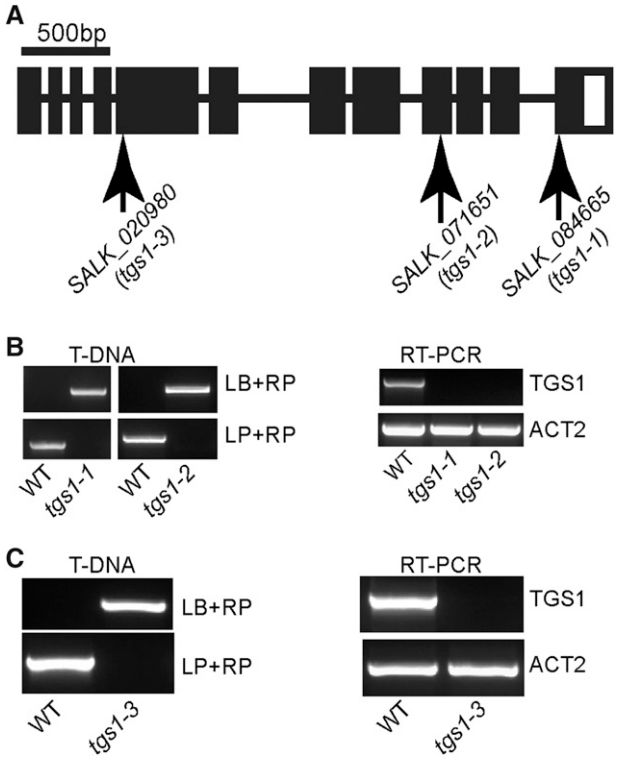

Figure 1. *TGS1* mutations confirmed. A, *TGS1* gene with T-DNA insertion sites indicated. Black boxes are exons, the white box is the 3′UTR; At1g45231 has no identified 5′UTR. B, Left, genotyping of *tgs1-1* and *tgs1-2* by T-DNA and gene-specific primers; right, shows RT-PCR analysis of *TGS1* transcript levels in wild type (WT), *tgs1-1*, and *tgs1-2* mutants. C, Similar analysis of chromosomal DNA and RT-PCR for *tgs1-3*.

type was successful, but no full-length transcript was detected in any of the T-DNA mutant lines (Fig. 1), indicating that the T-DNA insertion lines were null alleles.

At1G45231 Encodes a Homolog of Trimethylguanosine Synthase

SALK_084665, *SALK_071651*, and *SALK_020980* all interrupt At1G45231, whose predicted protein sequence is homologous to trimethylguanosine synthase of yeast (*S. cerevisiae*) and other organisms (Mouaikel et al., 2003). This Arabidopsis homolog to yeast TGS1 contains an RNA methyltransferase domain in its C-terminal region; 155 amino acids (residues 370–524; pfam09445) in this region are 39% identical to the yeast TGS1 methyltransferase domain (Fig. 2A). The Arabidopsis protein also has a long N-terminal region of 275 residues not present in the yeast TGS1 protein sequence. This N-terminal region contains a 23-amino acid domain identifiable as a "WW" domain (residues 169–192; Figure 2B) that is typically involved in protein-protein interactions (Otte et al., 2003). We named *SALK_084665 tgs1-1*, *SALK_071651 tgs1-2*, and *SALK_020980 tgs1-3*; we provisionally termed the protein AtTGS1 based on its sequence homology to other TGS1 proteins.

Localization of AtTGS1

When we analyzed the protein sequence of AtTGS1 using the cNLS Mapper algorithm (http://nls-mapper.iab.keio.ac.jp), a putative nuclear localization signal was identified between residues 507 and 537 (Fig. 2A). Submission of the protein sequence to the Plant Membrane Protein Database (http://aramemnon.uni-koeln.de) also indicated that TGS1 was likely targeted to the nucleus based on combined analysis of several independent prediction algorithms (Schwacke et al., 2007). To experimentally determine the location of AtTGS1 protein within plant cells, we created a GFP fusion to the C terminus of full-length AtTGS1 then cloned this AtTGS1-GFP fusion construct under control of the Cauliflower Mosaic Virus 35S constitutive promoter. When we transiently expressed the fusion in protoplasts of tobacco BY-2 cell lines and collected images by confocal microscopy, the GFP signal appeared highly concentrated in the nucleus and was also visible in the cytoplasm around the cell periphery (Fig. 3). When we treated the living protoplasts with Hoechst stain to identify nuclei and photographed them under UV illumination, the GFP and Hoechst fluorescence signals overlapped (Fig. 3), confirming that fusion of TGS1 to GFP caused it to be concentrated in the nucleus, although some AtTGS1-GFP remained in the cytoplasm.

AtTGS1 Is an Active Methyltransferase

Both yeast and human TGS1 proteins catalyze methyl transfer from *S*-adenosyl-Met to 7-methylguanosine 5′-diphosphate (m^7GDP) to form hyper-methylated $m^{2,7}$GDP in vitro (Hausmann and Shuman, 2005; Hausmann et al., 2008). To test whether Arabidopsis TGS1 was a functional ortholog of these proteins, we first assayed the methyltransferase activity of AtTGS1 in vitro. Repeated attempts to purify the protein from *Escherichia coli* engineered to express the full-length TGS1 protein failed; only insoluble inclusion bodies were produced. Instead, we fused the nucleotide sequence coding for the final 338 residues of AtTGS1 (residues 201–538), which includes the methyltransferase domain, augmented by addition of a C-terminal poly-His tag, to the C terminus of a DsRed protein coding sequence (Roston et al., 2011; Wang et al., 2012). When this fusion was expressed in *E. coli*, the protein proved amenable to purification using nickel affinity chromatography (Fig. 4A). We used this purified protein to investigate the methyltransferase activity using established methods. The in vitro reaction used radiolabeled free *S*-Adenosyl-L-Met, [methyl-^{14}C] and unlabeled m^7GDP, and the reaction products were analyzed by thin-layer chromatography followed by autoradiography (Fig. 4B). The in vitro reaction using the DsRed protein or boiled AtTGS1 produced no methyl

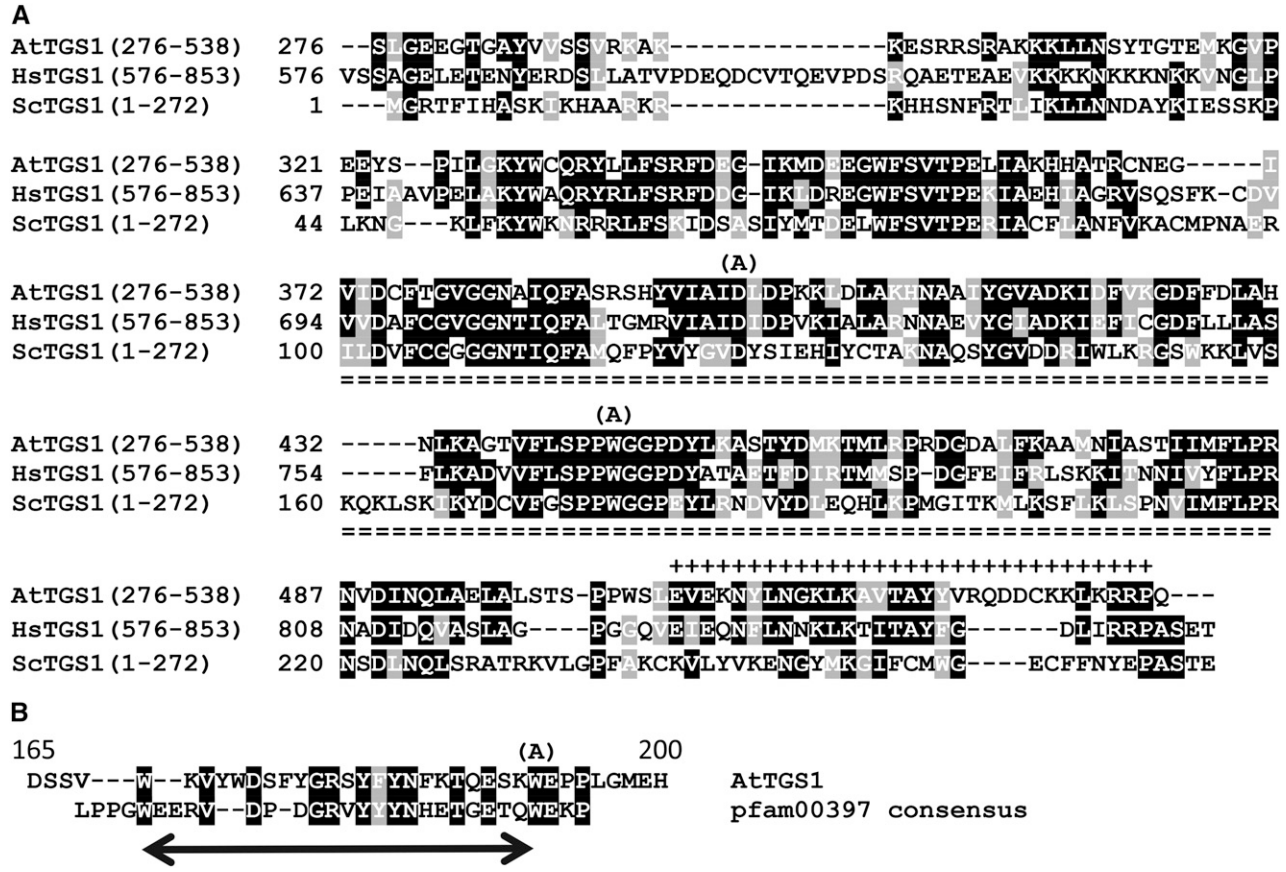

Figure 2. Sequence comparison of TGS1 proteins. A, Aligned portions of AtTGS1 with TGS1 from human (Hs) and yeast (Sc). The amino acid variants D397A and W444A are indicated by "(A)." The methyltransferase domain (pfam09445) of AtTGS1 is underscored by double lines, and the predicted nuclear localization signal is indicated by the plus signs. For AtTGS1, residues 276 to 538 are shown, and for HsTGS1 gene, the final 278 amino acids are shown. For ScTGS1, the final 43 residues of the sequence are not shown. B, The AtTGS1 sequence contains a WW domain, pfam00397. The introduced mutation W192A discussed in the text is indicated by "(A)," and the ΔWW (169–192) deletion is marked by the double arrow.

transfer to m^7GDP (Fig. 4B), but there was trimethylguanosine synthase1 activity in the reaction containing the DsRed-AtTGS1(201–538) fusion protein. The results show that the AtTGS1 protein methylated m^7GDP. When we repeated the assay with different controls, the AtTGS1 fusion protein methylated m^7GDP in parallel reactions with the human TGS1 protein (Supplemental Fig. S1).

AtTGS1 Complements *S. cerevisiae* Mutant *tgs1*Δ

TGS1 is vital to synthesis of methylated guanosine cap structures in yeast, and deletion of the single *tgs1* locus produces yeast that grow poorly at low temperatures (Monecke et al., 2009; Mouaikel et al., 2002). To test the functionality of AtTGS1 in vivo, we cloned the open reading frame representing the protein into the yeast constitutive expression vector pMK195 (Overvoorde et al., 1996) and transformed it into a yeast strain deleted in *tgs1* (*tgs1*Δ; Hausmann et al., 2008). Growth of *tgs1*Δ is similar to that of wild type at 28°C, but under cold conditions growth is inhibited, and at 18°C *tgs1*Δ yeast growth is severely retarded (Mouaikel et al., 2002). When we compared the growth of the *tgs1*Δ mutant yeast to the same strain except transformed with the AtTGS1 expression construct, AtTGS1 expression significantly recovered the ability of the yeast to grow at 18°C (Fig. 5). To confirm that complementation of the yeast cold growth inhibition was caused by methyltransferase activity of AtTGS1, we introduced mutations at conserved residues (Hausmann et al., 2008) in the methyltransferase domain, D397A and W444A (Fig. 2). Neither of these variant proteins complemented the inhibited growth of yeast *tgs1*Δ at 18°C (Fig. 5); AtTGS1 not only complements yeast *tgs1*Δ phenotype but does so dependent on amino acids required for methyltransferase activity.

Homology of the 538 amino acid protein sequence of AtTGS1 to the yeast and human TGS1 proteins is strong in the C-terminal portion of the protein, including the methyltransferase domain (39% identity to the yeast methyltransferase domain; Fig. 2A). However, N-terminal region of the Arabidopsis protein includes 276 amino acid residues with no homology to the much shorter yeast

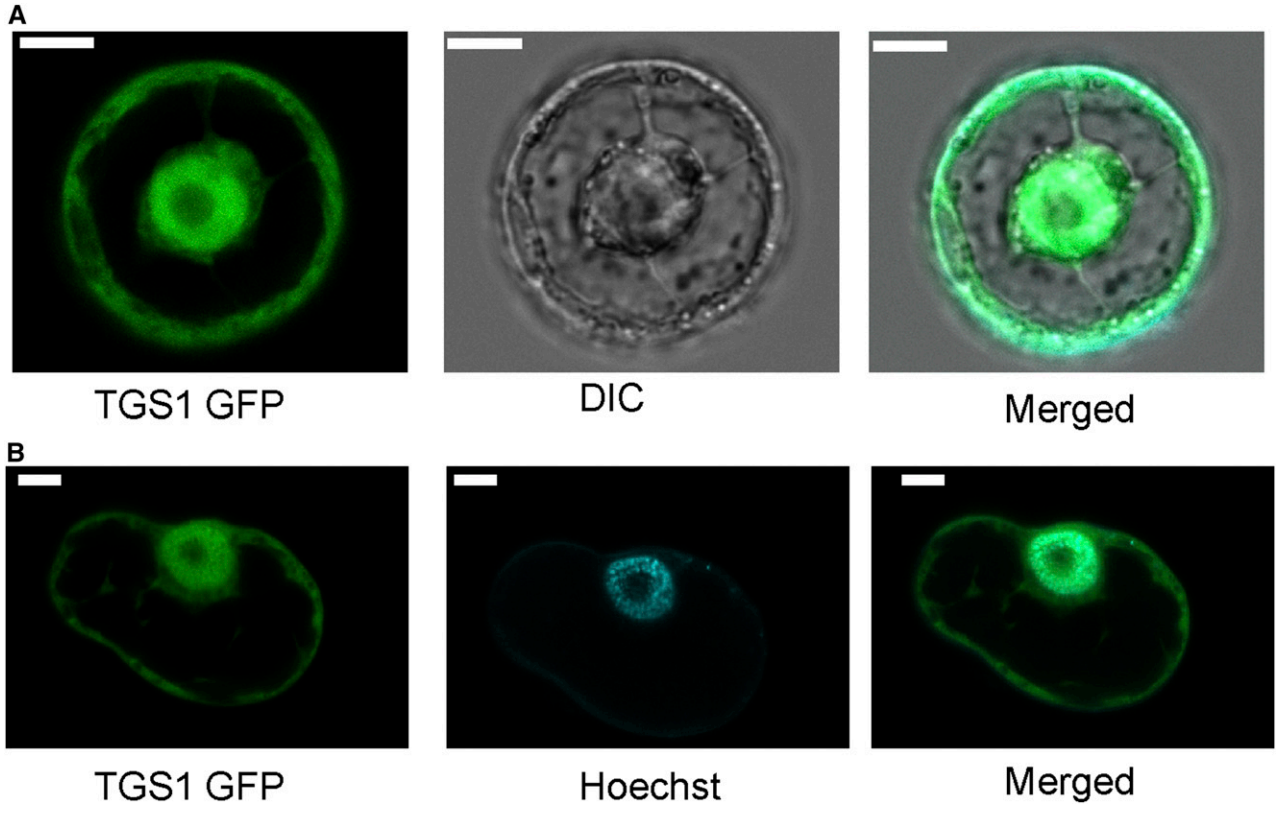

Figure 3. Localization of AtTGS1. AtTGS1-GFP protein was transiently expressed in protoplasts of tobacco *BY-2* cell lines under the 35S constitutive viral promoter; images were collected by confocal microscopy. A, GFP, differential interference contrast (DIC) image, and GFP-DIC are left, middle and right, respectively; B, GFP, Hoechst 3342 fluorescence, and overlap of those two is shown in left, middle, and right, respectively. Bars = 10 μm in A and 7.5 μm in B.

sequence. Human TGS1 also has an N-terminal sequence without homology to the yeast sequence, in this case 575 amino acids long, although there is no detectable homology between the human and Arabidopsis N-terminal regions (<20% identity). Within the Arabidopsis N-terminal region, amino acids 169 to 192 encode a WW domain, recognized by amino acid homology to other proteins (Bedford et al., 2000). When we created a specific *AtTGS1* variant that removed the WW domain (amino acids 169–192; AtTGS1ΔWW), expression of the variant protein still complemented the *tgs1*Δ mutation and relieved the inhibition of yeast growth at 18°C (Fig. 5), demonstrating that the activity of the WW domain was inessential to AtTGS1 cold growth restoration in yeast.

Phenotypic Analysis of *tgs1* Mutants

To examine the details of the *tgs1* growth defect throughout the Arabidopsis growth cycle, we cultivated wild-type and *tgs1* plants under both normal and chilling conditions. None of the *tgs1* mutants had any visible vegetative phenotype when grown at 22°C. The *tgs1* mutants grew normally with no leaf distortion or lesions. Seed germination, establishment on soil, plant size, time of flowering, the development of *tgs1* buds and flowers, and seed set were the same as in wild type (Fig. 6), and they senesced at the same time as wild-type plants. We used fluorescence analysis (Wu et al., 1997) to measure the potential quantum yield of PSII (F_v/F_m) for rosette leaves of plants growing at 22°C. The results indicated no significant difference between wild type (F_v/F_m = 0.82 ± 0.03) and *tgs1-1* (F_v/F_m = 0.81 ± 0.01, both SE; n = 5). We measured the growth rate of the plants by collecting the above-soil portions of three to five plants at intervals over their growth to maturity, weighed the tissue, and constructed a growth curve based on the average fresh weight of the aerial portions. The results showed that growth of the mutant and wild type were equal at 22°C (ω^{-1} = 0.21, ±0.03; Fig. 6E). We measured seed yield for the wild type and two *tgs1* mutants and found that at 22°C the mutants produced seed at levels comparable to the wild type (wild type 0.27 mg/plant, *tgs1-1* 0.23 ± 0.02, *tgs1-2* 0.27 ± 0.02 SE; $n \geq 28$ plants).

To characterize the chilling sensitivity of the *tgs1-1* mutants, we first used the same chilling regimen as for our original screen: Wild-type and mutant seedlings were grown at 22°C for 10 d then transferred to 5°C. After 20 d at the lower temperature, mild defects in both

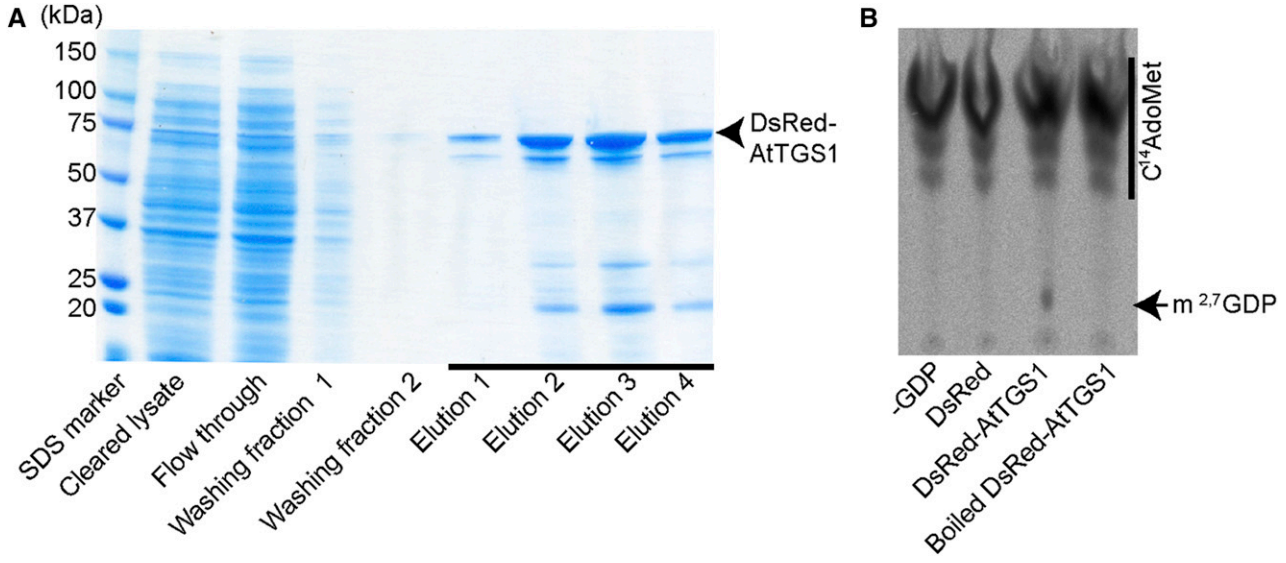

Figure 4. Purification and methyltransferase activity of recombinant AtTGS1. A, Fusion of His-DsRed to the C-terminal AtTGS1(201–538) of TGS1, which includes the methyltransferase domain, was purified from *E. coli* by nickel-affinity chromatography; SDS-PAGE analysis of elution fractions is shown. Protein sizes of the standard are indicated at the left. B, Activity of purified AtTGS1 fragment in vitro. The fusion protein produces methylated GDP, but neither the DsRed protein alone nor the boiled DsRed-TGS1 controls are active. Free *S*-adenosyl-L-Met, [methyl-^{14}C] substrate forms a large mass at the top, while the methylated GDP forms a lower band on the thin-layer chromatography plate, marked by the arrow.

tgs1-1 and *tgs1-2* were evident; mutant leaves were clearly smaller than those of wild type (Fig. 7A). The plants continued to grow at 5°C, and after a total of 35 d in the cold, the *tgs1* mutants were significantly smaller than wild-type plants, and their leaves were not only much smaller but sickly in appearance; young leaves were more curled than in wild type, and old leaves were bleached and brown compared to wild-type leaves (Fig. 7, B and C). Leaf senescence in mutant lines also appeared much earlier than in wild-type plants (Fig. 7; Supplemental Fig. S3). However, both wild-type and *tgs1* mutant plants survived the prolonged cold treatment. Measurements of fresh weight of the above-ground portions of the plants under chilling conditions showed a clear difference in growth rate between the mutant and the wild type when the plants were cultivated at 5°C, with ω^{-1} of wild type 0.070 ± 0.06, and of *tgs1-1* 0.044 ± 0.004 (Fig. 7D). When the *tgs1* plants had been grown in the cold for a total of 150 d, the wild-type plants were much larger and produced normal buds, flowers, and seeds. The *tgs1* mutant plants were very small and sickly, and the buds and flowers were defective; no seeds were produced from the mutant plants after 150 d at 5°C (Fig. 8A).

To test whether these *tgs1-1* bud and flower defects simply resulted from the small and sickly vegetative phenotype, we grew both the mutant and wild-type plants at 22°C for 45 d, rather than just 10 d, before subjecting them to chilling stress at 5°C. Under this regimen, *tgs1-1* plants still produced smaller rosettes with smaller individual leaves than wild type, but the vegetative parts of the plants appeared healthy throughout their growth. After 51 d of growth at 5°C, all plants produced buds and flowers. However, the buds and flowers of the mutant appeared to be much smaller than those of wild type and defective in form (Fig. 8B; Supplemental Fig. S3A), demonstrating that AtTGS1 is specifically important to bud and flower development under chilling conditions. To determine whether the *tgs1* mutant phenotype could be seen at temperatures above 5°C, the wild type and *tgs1* mutant were grown at 10°C for 90 d after a 12 d preparatory growth at 22°C. The *tgs1-1* mutant plants were slightly smaller, and the plants had shorter stems than wild type. However, the *tgs1-1* plants finished their life cycle normally, with flowers exhibiting minor defects compared to wild type (Fig. 8C; Supplemental Fig. S3B).

Expression of TGS1 Relieves *tgs1-1* Chilling Sensitivity

We constructed a plant transformation vector to express the AtTGS1 open reading frame under control of its native promoter. After we transformed *tgs1-1* plants with this construct, we confirmed the presence of the *TGS1* expression cassette by PCR. Three independent transgenic lines were analyzed by RT-PCR to confirm expression of the *TGS1* construct. When these lines were subjected to chilling at 5°C, they displayed normal wild-type plant size, larger than the *tgs1-1* mutant plants, and remained as healthy as the wild-type plants (Fig. 9), demonstrating that expression of AtTGS1 overcomes the chilling sensitivity produced by the T-DNA insertion in At1g45231. We similarly expressed a variant of TGS1

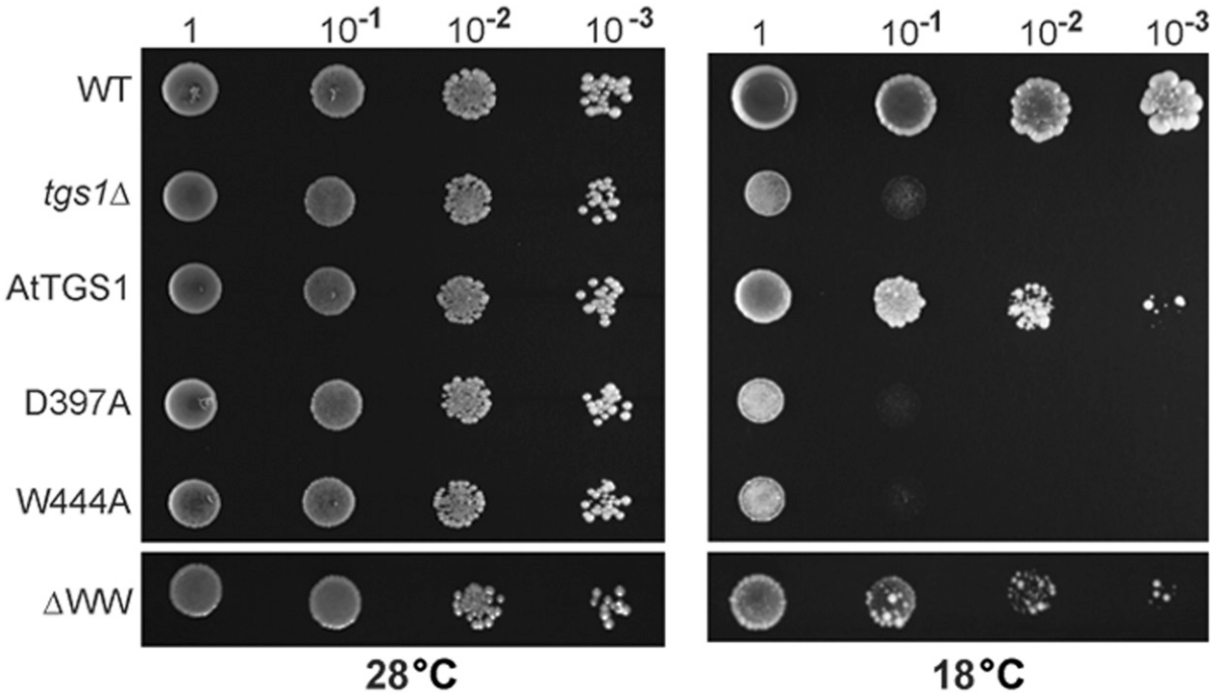

Figure 5. Arabidopsis TGS1 expressed in *tgs1*Δ yeast. Wild-type (WT) yeast, top, grows well at either 28°C (left) or 18°C (right). Yeast lacking TGS1 (*tgs1*Δ) grow like wild type at 28°C but fail to grow at 18°C. Expression of the AtTGS1 protein restores *tgs1*Δ to substantially wild type growth at 18°C. When expressed proteins have mutations in the methyltransferase domain, AtTGS1(D397A) and (W444A) yeast fail to grow at 18°C. Expression of AtTGS1 deleted in the WW domain, AtTGS1ΔWW, still confers ability of the yeast mutant to grow in the cold. Both wild-type and *tgs1*Δ yeast were transformed with empty pMK195 vector for this experiment. The AtTGS1ΔWW clone was analyzed simultaneously with the others but on a separate media plate. For each strain, 20 μL of an overnight culture adjusted to OD = 1.0 was spotted on the plate, along with 10-fold dilutions of each culture as indicated.

into which we had introduced a mutation, W192A, disrupting the WW domain found in the TGS1 N-terminal sequence (Fig. 2), and a second variant, TGS1ΔWW, which completely removed the conserved WW domain (Fig. 2). Expression of either the W192A variant or the AtTGS1ΔWW construct equally overcame the chilling sensitivity of *tgs1-1* (Supplemental Fig. S4), demonstrating that the WW domain is not essential for *TGS1* complementation of the *tgs1-1* chilling-sensitive phenotype and providing further evidence that the chilling-sensitive phenotype is caused by the mutation at *tgs1.*

DISCUSSION

Chilling is not always detrimental to plants; the physiology of temperate plants is not only able to adapt to cold, leading to increased freezing tolerance (Knight and Knight, 2012; Miura and Furumoto, 2013), but many plants even rely on cold weather both to correctly time bud dormancy and to achieve proper germination and reproduction (Holdsworth et al., 2008; Penfield and Springthorpe, 2012). However, important crops have been introduced into temperate climes from tropical or subtropical habitats and are subject to reduced growth and tissue damage from chilling temperatures (Lyons, 1973; Wang, 1990; Lukatkin et al., 2012; Gao et al., 2015; Barrero-Gil et al., 2016). This chilling sensitivity has major effects on world food supplies (Vinocur and Altman, 2005; Thakur et al., 2010), affecting tomato, cucumber, maize, rice, cotton, and a host of other crops (Paull, 1990). Determining which genes are important to chilling sensitivity may lead to amelioration of chilling damage and could be a key step in converting sensitive crops to chilling-tolerant ones, either by molecular breeding or by molecular-genetic modification.

However, chilling produces a response in hundreds of genes (Thomashow, 2010; Zinn et al., 2010), and we are still far from understanding the totality of loci important to chilling sensitivity. The molecular and genetic tools available for the chilling-tolerant plant Arabidopsis make it a powerful resource for identifying chilling sensitivity determinants (Provart et al., 2016). Mutation followed by phenotypic screening for cold-sensitive Arabidopsis can identify determinants that are different between cold-tolerant and cold-sensitive plants. Indeed, several key loci important to chilling sensitivity have been previously identified through Arabidopsis screens (Schneider et al., 1995; Tokuhisa et al., 1997, 1998; Truernit et al., 2008).

Here, we report an initial screen of 3739 individual Arabidopsis lines with indexed T-DNA insertions

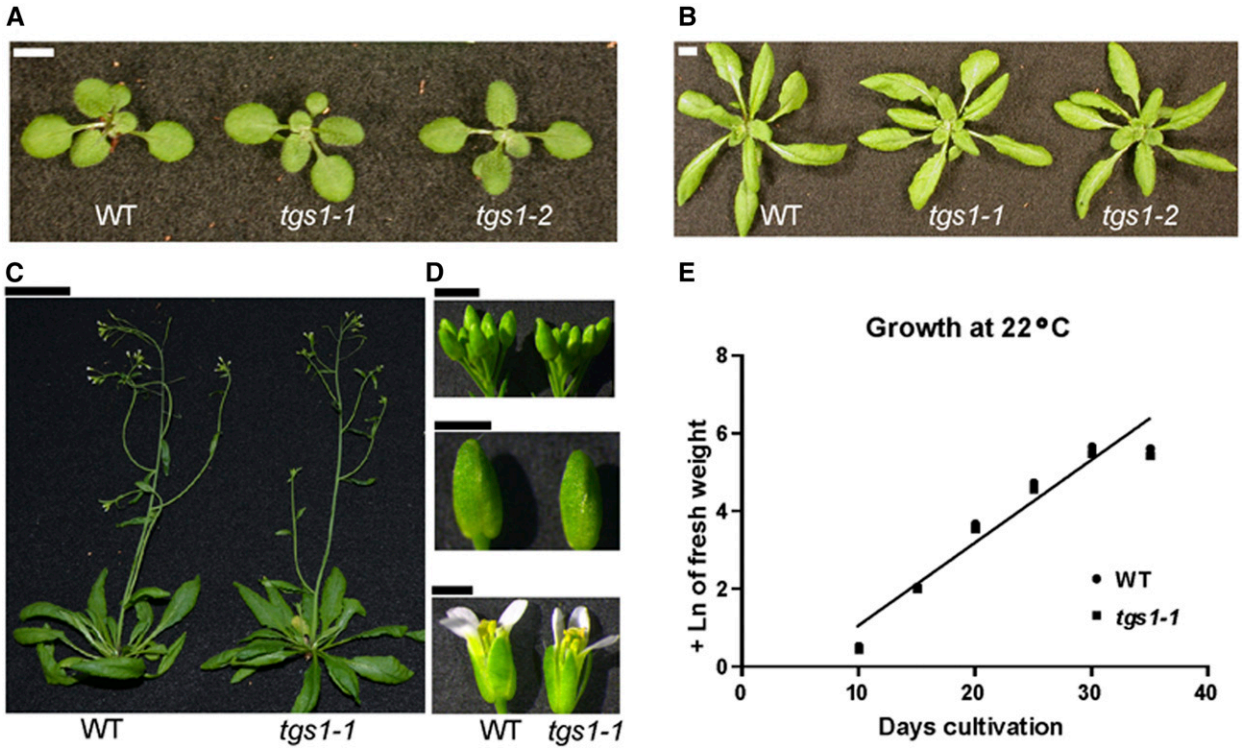

Figure 6. Growth and reproduction of *tgs1* mutants at 22°C. A, Plants were grown at 22°C for 12 d; B, 22°C for 21 d total. C, Wild type (WT) and *tgs1-1* after 22°C for 32 d. D, Flowers of plants in C. Clusters of flower buds, a single flower bud, and mature flowers. E, Mutant *tgs1-1* and wild-type plants have the same growth rate, as measured by fresh weight; the growth rate (ω^{-1}) for each plant line is 0.21, ± 0.03. Bars = 1 cm in A and B, 4 cm in C, and 1 mm in D.

(Alonso et al., 2003) for plants that are phenotypically wild type at 22°C but suffer damage or reduced growth at 5°C. To date, our screen has identified 29 putative mutants with these characteristics (Supplemental Table S1). We focused on one line, SALK_084865, which contains a T-DNA insertion in At1G45231. When two additional T-DNA insertional alleles in the gene exhibited the same chilling-sensitive phenotype, we decided to characterize the role of the encoded enzyme, TGS1, in low-temperature growth of the plant.

All three homozygous mutant *tgs1* insertion lines grew normally at 22°C (Fig. 6). They showed leaf development, color, and shape were indistinguishable from that of the wild type. When we measured the potential quantum yield of PSII, it was also essentially the same as wild type, and the leaves aged as did those of the wild type, without yellowing or formation of lesions. A growth curve based on measurements of above-soil fresh weight demonstrated that mutant growth was equivalent to wild type at 22°C (Fig. 6). As the plants reached maturity, they were the same size and bolted at the same time as wild type. The formation of flower clusters, maturation of individual flowers, and set of seed were all the same as seen in wild-type plants at normal 22°C temperature (Fig. 6).

The *tgs1* mutants were dramatically impaired during the chilling-sensitive screening protocol, when they were transferred to 5°C for 150 d after preliminary growth at 22°C (Figs. 7 and 8). The leaves were both very small and deformed in shape and the rosettes tiny. The leaves of the mutant turned yellow long before those of the wild type, and necrosis developed at the leaf margins (Fig. 7; Supplemental Fig. S2). Even when we delayed the chilling stress until the plants were 45 d old, the individual leaves of the mutant were clearly smaller as they continued to grow at 5°C, producing smaller rosettes (Supplemental Fig. S3). An additional growth experiment that transferred plants to 10°C after 12 d at 22°C produced plants that were smaller than the wild type but healthy (Supplemental Fig. S3). When we created transgenic plants expressing the TGS1 coding region under control of its native promoter, the chilling defects of the *tgs1* mutation were relieved (Fig. 9), establishing that in Arabidopsis *TGS1* expression is pivotal to chilling tolerance. The *tgs1* phenotype was equally relieved by expression of the alternate forms of *tgs1* either mutated (W192A) or deleted (Δ169–192) in the WW domain sequence (Fig. 2), indicating that this sequence is not required for chilling resistance (Supplemental Fig. S4).

Disruption of flower development was especially evident in *tgs1* mutants grown at 5°C. Under the conditions of the original screen, the flowers were extremely small and obviously deformed in structure, and neither petals, stamens, nor pistils formed normally (Fig. 8A); *tgs1* mutant

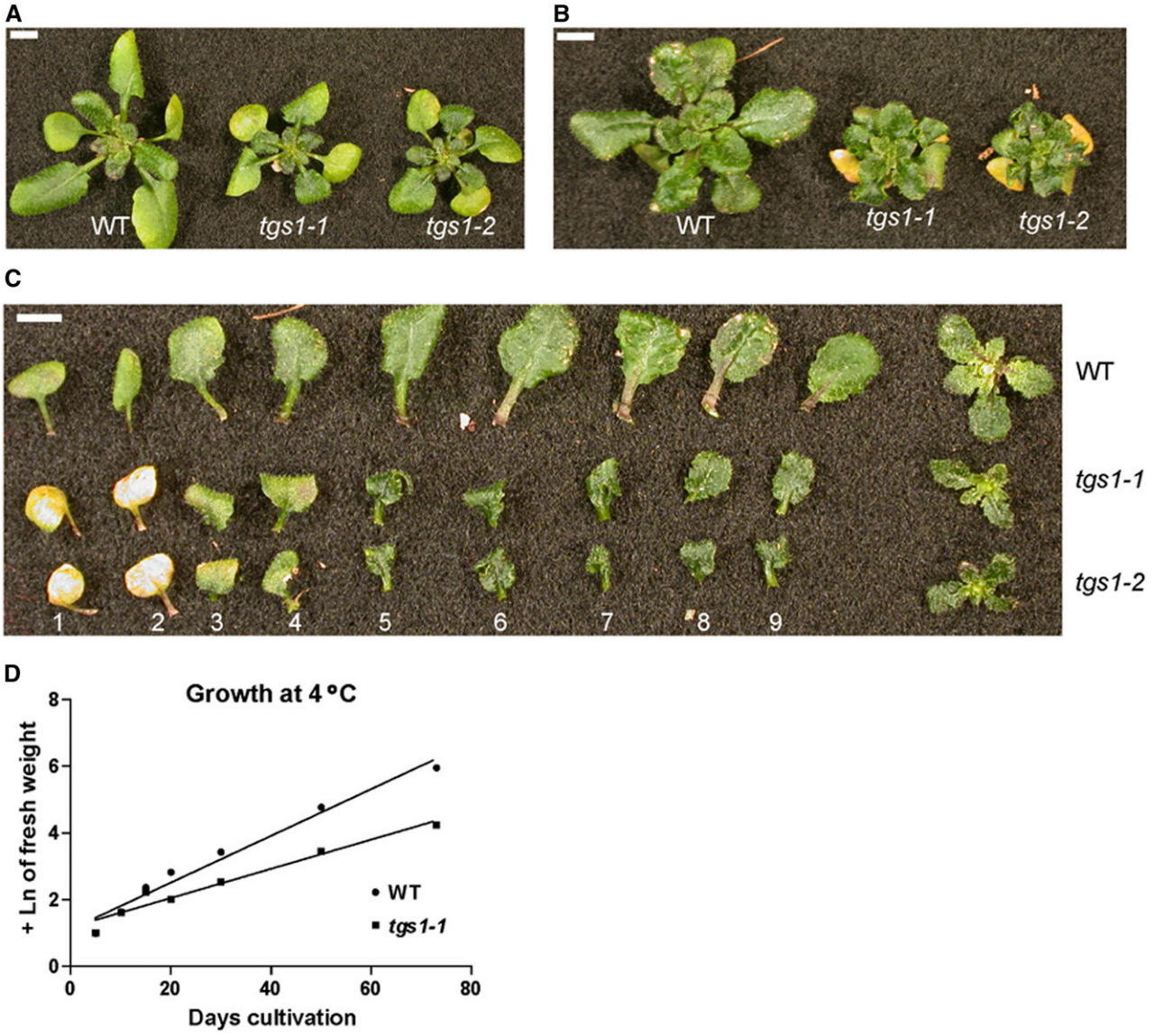

Figure 7. Vegetative growth of *tgs1* mutants at 5°C. A, Plants grown at 22°C for 12 d followed by 5°C for an additional 20 d; B, and C, continued growth at 5°C for an additional 15 d. In C, the leaves are numbered by their appearance, with the first true leaf as 1; leaves numbered 5 through 9 were produced under chilling conditions. The residue of the rosettes after leaf removal is shown at the right. D, Mutant *tgs1-1* and wild-type plants have different growth rates, as measured by fresh weight, at 5°C. The growth rate (ω^{-1}) of *tgs1-1* was 0.044 ± 0.004, much less than wild-type rate of 0.070 ± 0.006. Bars in the photographs indicate 1 cm.

plants produced no seed under long-term chilling treatment. When we examined growth after 45 d of 22°C growth followed by a shift to 5°C, leaf damage was reduced but *tgs1* flower development was still aberrant (Fig. 8B). Growth and reproduction largely recovered when plants were cultivated at 10°C, although the flowers of these small plants had minor defects (Fig. 8C).

Correct intracellular targeting is important to TGS1 function; analysis of mutant forms of yeast and human TGS1 proteins that are incorrectly targeted show reduced trimethylation activity (Boon et al., 2015). Sequence analysis of the predicted AtTGS1 protein indicated that it might be targeted to the nucleus, and when we expressed a TGS1-GFP fusion protein in tobacco cells, nuclear targeting was evident, although some protein also appeared outside the nucleus (Fig. 3). In yeast, TGS1 is primarily located in the nucleolus (Mouaikel et al., 2002), but the targeting of Arabidopsis TGS1 is more like that seen in metazoans, where TGS1 has been detected both in the nucleus and the cytoplasm (Zhu et al., 2001; Enünlü et al., 2003; Komonyi et al., 2005).

The AtTGS1 protein is a sequence ortholog of the other TGS1 proteins in the highly conserved RNA methyltransferase domain common to both yeast and human TGS1 proteins (Mouaikel et al., 2002, 2003). The domain was easily recognized within the C-terminal

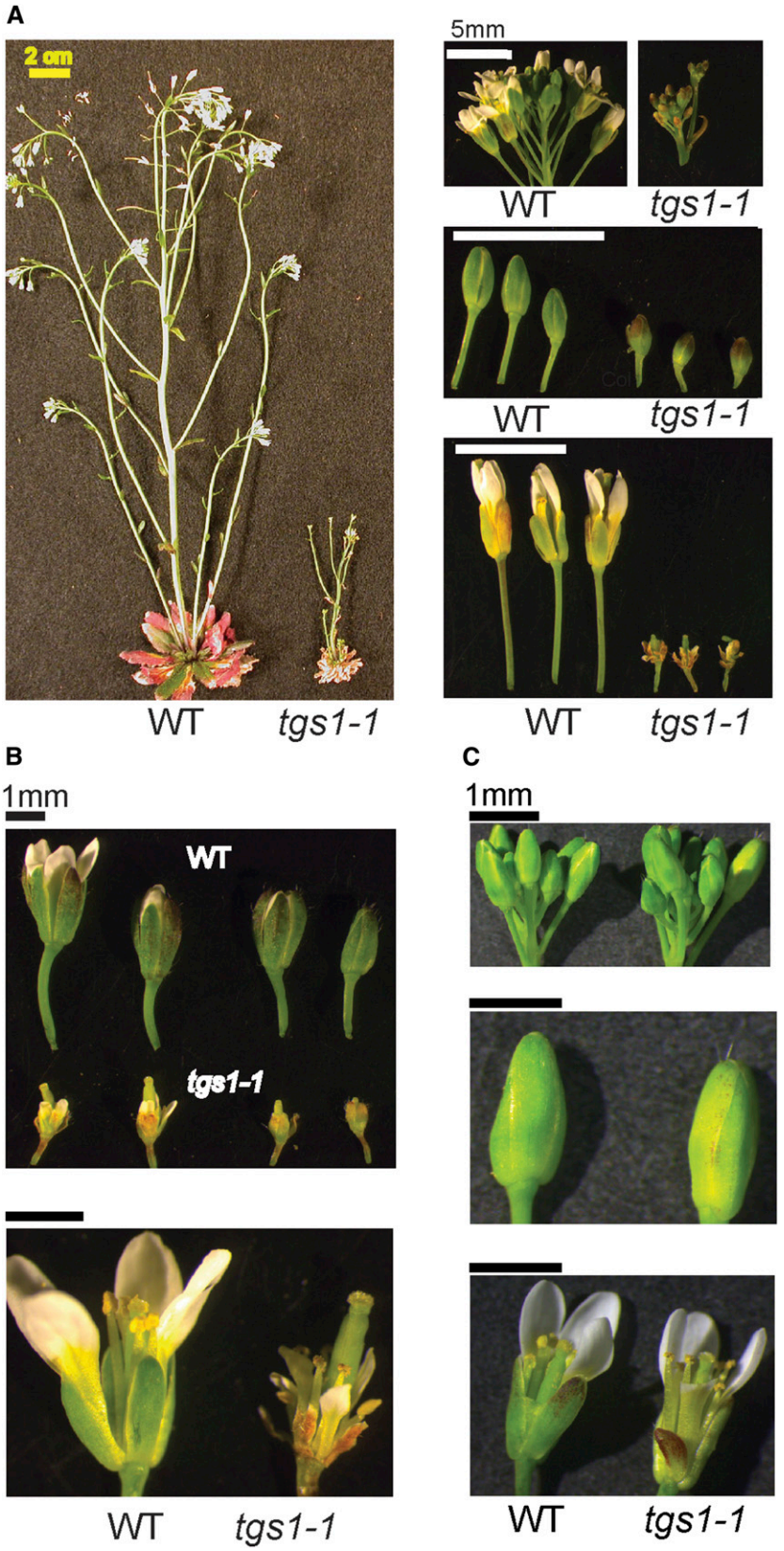

Figure 8. Development and reproduction of *tgs1-1* under chilling conditions. A,Wild type and *tgs1* mutant plants grown at 22°C for 12 d, followed by 150 d at 5°C. Left, whole plants; right, full flower clusters, developing flower buds, and mature flowers. B, Plants grown at 22°C for 45 d, followed by 51 d at 5°C. C, Plants grown 12 d at 22°C followed by 90 d at 10°C. Full flower cluster, developing flower buds, and mature flowers. Photos of the whole plants for B and C are in Supplemental Figure S3.

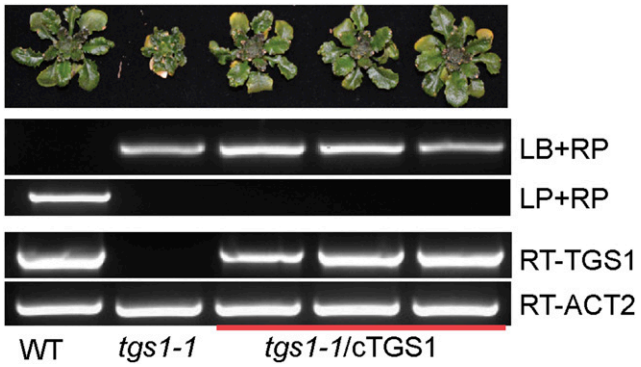

Figure 9. Transgenic expression of *TGS1* in *tgs1-1*. Top, phenotype of indicated plants under 5°C cultivation. Genotyping shows that *tgs1-1* and three independent transgenic lines were homozygous at At1g45231 (middle). TGS1 transcript is absent in *tgs1-1*, and transcript restoration by transgenic expression (bottom) relieves the chilling phenotype.

260 amino acids of AtTGS1 (Fig. 2). To determine if the Arabidopsis protein was also a functional TGS1 ortholog, we first demonstrated its activity using an in vitro assay. We were unsuccessful in purifying full-length AtTGS1 from an *E. coli* expression system, similar to the difficulty reported with expressing the full-length human protein (Hausmann et al., 2008). The difficulty purifying the human protein may be due to its long N-terminal extension, which mediates self-association (Boon et al., 2015); the AtTGS1 protein also has an N-terminal extension of 275 residues with no recognizable homology to human TGS1. When we expressed a fusion of the C-terminal 338 residues of AtTGS1 to DsRed in *E. coli* and purified the protein (Fig. 4A), it was an active trimethylguanosine synthase (Fig. 4B). The AtTGS1 fragment represents the region of the protein most conserved in TGS1 protein family (Fig. 2), with strong homology to the fragment of the human protein used to establish its in vitro activity (Supplemental Fig. S2).

We also tested TGS1 activity in vivo by expressing AtTGS1 in a *S. cerevisiae* strain deleted for *tgs1*. The *tgs1*Δ cold-growth inhibition (Hausmann et al., 2008) was relieved by expression of AtTGS1 (Fig. 5). Conservation of sequence in the methyltransferase domain allowed us to specifically mutagenize conserved residues D397A and W444A (Fig. 2), (Hausmann et al., 2008), and the resulting mutant proteins failed to relieve the yeast cold-growth inhibition. These results demonstrate that the rescue of yeast cold growth at 18°C was dependent on the conserved methyltransferase domain of AtTGS1 (Fig. 5). A recognizable protein interaction domain, termed a WW domain (Macias et al., 2002), was identified between residues 169 and 192 in AtTGS1 (Fig. 2B). When we expressed a form of AtTGS1 that was full-length except for specific deletion of the amino acids of this domain, AtTGS1ΔWW, expression of the deleted construct still permitted yeast growth at cold temperature, demonstrating that presence of the conserved WW motif was not required to complement the yeast cold-growth inhibition (Fig. 5).

A hypermodified 2,2,7-trimethylguanosine (TMG) cap structure terminates many noncoding RNAs in eukaryotic species, including those of plants (Ghosh and Lima, 2010). TMG cap formation depends on TGS proteins and plays a key role in biogenesis of both small nuclear RNA (snRNA) and a subset of small nucleolar RNA (snoRNA), molecules that have important roles in a wide range of cellular functions (Burroughs et al., 2014). Although plant homologs to yeast and animal TGS1 proteins have been noted (Mouaikel et al., 2002) and expression analysis of one homolog conducted (Siena et al., 2014), there has previously been no characterization of TGS1 in plants.

TGS1 mutants of other organisms have been analyzed. In yeast, deletion of *tgs1* eliminates the TMG caps on snRNAs important to splicing of premRNA, and on some snoRNAs that are normally hypermethylated for maturation of prerRNA (Mouaikel et al., 2002); yeast TGS1 protein is found concentrated in the nucleolus, and its location is important to its snoRNA methylation activity (Boon et al., 2015). Yeast TGS1 plays an additional role in methylation of telomere RNA (Franke et al., 2008; Tang et al., 2012). Notwithstanding its roles in all these functions, the yeast *tgs1Δ* phenotype is confined to inhibited growth in the cold (Mouaikel et al., 2002) and failure to sporulate (Qiu et al., 2011). Unlike yeast *tgs1Δ*, loss of TGS1 has dire consequences for multicellular animals. Mutation of TGS1 (T08G11.4) in *Caenorhabditis elegans* causes larval lethality (Zipperlen et al., 2001). *Drosophila* TGS1 is required for adult viability in both muscle and neurons (Komonyi et al., 2005; Provart et al., 2016), and loss of TGS1 function is lethal in the pupal stage. Disruption of *tgs1* in mice similarly caused early embryonic lethality (Jia et al., 2012), establishing that TGS1 proteins are essential for many higher organisms.

It is therefore somewhat surprising that neither growth nor reproduction of Arabidopsis *tgs1* mutants is altered at regular growth temperatures; these plants grow at the same rate as wild type and proceed normally through their vegetative and reproductive life cycle (Fig. 6). One explanation for survival of *tgs1*mutants may be that some functions of TGS1 in plants apparently differ from other organisms. Arabidopsis and other plants have abundant small nucleolar snoRNAs (Brown et al., 2003), but these have gamma-monomethyl phosphate caps, unlike the TMG caps of metazoans (Shimba et al., 1992); their activities are likely independent of TGS1 activity. This accords with proteomics data, which does not identify AtTGS1 in the nucleolus (Brown et al., 2005; Pendle et al., 2005), and with the results of our GFP fusion analysis, which showed no nucleolar concentration of TGS1 (Fig. 3). Telomere maintenance in Arabidopsis is also different from in animals, since telomerase is expressed only in meristem tissue, not in all tissues as for metazoans. Arabidopsis mutants without telomerase exhibit no dramatic phenotypic defects until the seventh generation, and viable seed are produced at least until the ninth generation (Riha et al., 2001), a much slower response to telomere loss than in mice (Amiard et al., 2014).

In addition to the functional differences enumerated, a second explanation for survival and growth of *tgs1* mutants at normal temperatures is the presence of a TGS1 homolog in Arabidopsis that may provide partial functional overlap with TGS1. There is a homologous protein sequence encoded At1g30550 in the Arabidopsis genome, and the presence of two TGS-like genes is widespread in the plant kingdom (Mouaikel et al., 2003), including both chilling-resistant and chilling-sensitive plants. However, activity of this homolog clearly is insufficient under chilling conditions to support normal growth and reproduction of Arabidopsis *tgs1* mutants.

One function of TGS1 shared with yeast and animals is the hypermethylation of snRNA required for correct splicing of premRNA to mRNA. Indeed, the cold-growth inhibition of *S. cerevisiae tgs1*Δ has been attributed to specific failures of premRNA splicing (Qiu et al., 2012; Qiu et al., 2015). Arabidopsis RNA splicing mechanisms have been thoroughly described (Meyer et al., 2015), and alternative splicing of mRNA is an important regulator of plant responses to a host of environmental stresses, including high light, heat, cold, high salt, and dehydration (Filichkin et al., 2010; Capovilla et al., 2015). For cold stress in particular, alternative splicing events were abundant, and expression of splicing factor proteins that promote alternative splicing was induced by the cold (Iida et al., 2004; Capovilla et al., 2015). Furthermore, temperature changes affect the splicing patterns of the splicing regulators themselves (Lazar and Goodman, 2000; Palusa et al., 2007). Indeed, alternative splicing can be seen in ambient temperature shifts from 20°C to only 16°C (Streitner et al., 2013), indicating that changes in splicing may be critical to the ability of plants to adjust to cold. The fact that the Arabidopsis *tgs1* mutants produce defective flowers in chilling conditions (Fig. 8) may be due to the importance of alternative mRNA splicing in floral development (Jiao and Meyerowitz, 2010; Swaraz et al., 2011; Wang et al., 2014).

The genetic methods we employed here hold the promise of rapidly identifying other novel chilling stress genes by analysis of more T-DNA lines. Since TGS1 is found in all plants, including cold-sensitive ones like rice, further analysis of the locus has the potential to direct crop modification by molecular breeding or by transgenic alteration to convert chilling-sensitive crops to more chilling-resistant varieties.

MATERIALS AND METHODS

Plant Material and Growth

Arabidopsis (*Arabidopsis thaliana*) ecotype Col-0 was used as wild-type control. Seeds were usually sown directly on soil or on Murashige and Skoog plates after sterilization. The sown seeds were incubated at 5°C for 48 h, then cultivated at 22°C with 16 or 24 h light at 100 to 150 $\mu E/m^2$ unless otherwise detailed in the text. For chilling treatment, after the plants geminated and grew 12 d at 22°C, the plants were transferred to 5°C with continuous light for as long as 150 d, or other periods as indicated in the text. Details of the Salk T-DNA collection employed can be obtained from the ABRC (https://abrc.osu.edu), stock CS27943, part of Joseph Ecker's SALK confirmed T-DNA project (Alonso et al., 2003). The seed stock consists of 3739 independent confirmed SALK lines, one confirmed allele per line. Individual insertion lines Salk_084665 (*tgs1-1*), Salk_071651 (*tgs1-2*), and Salk_049230 (*tgs1-3*) were obtained from ABRC.

Screen for Chilling-Sensitive Plants

For the primary screen, seeds from each independent seed stock were sown directly on soil. For each insertion line, 10 to 15 seeds were planted in three groups, and after germination, one healthy plant from each of the groups was chosen for analysis and the remainder culled. After 12 d at 22°C under 24 h light, plants were transferred to 5°C for an additional 8 to 12 weeks. All the plants exhibiting a visible phenotype in normal and chilling conditions were subjected to further analysis by repeating the original screening process for the selected lines. The Arabidopsis Information Resource (http://www.arabidopsis.org/) was queried for all candidate loci exhibiting phenotypes in this secondary screen, and those whose function was well characterized were not further examined (Supplemental Table S1). The remaining lines were evaluated as to whether the T-DNA insertion was located in the 5′UTR of a gene or in an intron or exon (Supplemental Table S1). Additional alleles of candidate loci were ordered from ABRC when available. Phenotypic analysis of additional alleles was conducted as for the initial screen.

Sequences and Analysis

Sequence data were obtained from The Arabidopsis Information Resource under the following Arabidopsis Genome Initiative numbers: AtTGS1 (At1g45231) and its homolog described in the text (At1g30550). Additional sequences are from GenBank (https://www.ncbi.nlm.nih.gov); the accession number for AtTGS1 is AEE32102.1, the AtTGS1 homolog is AEE31243.2 and AEE31242.2. The human (*Homo sapiens*) TGS1 protein sequence is NP_079107, and the *Saccharomyces cerevisiae* TGS1 gene is identified by AJW12023.1. Sequence homology and figure preparation used Geneious R6.1.8 (Biomatters).

DNA Extractions and RT-RCR

DNA for PCR analysis was obtained by a method adapted from (Edwards et al., 1991). In brief, 10- to 20-mg pieces of leaf tissue were sampled from 3-week-old Arabidopsis plants and thoroughly ground in 180 μL extraction buffer (200 mM Tris HCl, pH 7.5, 250 mM NaCl, 25 mM EDTA, 0.5% SDS) using a plastic pestle. The DNA was precipitated by adding 400 μL 95% ethanol directly to the ground sample, followed by centrifugation at 18,000 RCF for 5 min. The pellet of leaf debris and DNA was air-dried for 10 min to remove the ethanol, then dissolved in 100 μL TE buffer (10 mM Tris-HCl and 1 mM disodium EDTA, pH 8.0). A second centrifugation at 18,000 RCF for 1 min pelleted the leaf debris, and 1 μL of the supernatant was used as template in PCR reactions that used GoTaq DNA Polymerase (Promega) and appropriate primers (Supplemental Table S2). Total RNA was likewise purified from 3-week-old Arabidopsis leaves using the RNeasy plant mini kit (Qiagen), including the on-column DNase digestion (RNase-free set; Qiagen) to eliminate DNA contamination as recommended by the manufacturer. First stand cDNA synthesis with SuperScript III (Invitrogen) was followed by PCR analysis with the primers for ACT2 as internal control.

TGS1 Localization by Transient Protoplast Assay

The primers used for in this research are listed in Supplemental Table S2. The thermostable polymerase used for amplification was KOD polymerase (Takara), except as otherwise noted. After PCR amplification of the TGS1 open reading frame, the amplified product was cloned into pENTR/D-TOPO vector (Invitrogen) and the sequence of a clone verified. This sequence was transferred to vector pB7WG2 (Karimi et al., 2002) via an LR-Clonase reaction (Invitrogen), creating an AtTGS1-GFP fusion open reading frame under control of the viral 35S promoter. AtTGS1-GFP was transiently expressed in protoplasts of tobacco BY-2 cell lines (Miao and Jiang, 2007), and images of the protein localization were photographed using a Leica SP-8 confocal microscope. Hoechst 33342 (1 μL of a 10 mg/mL solution) was added to each sample to stain nuclear regions of the transgenic living protoplasts.

Purification of AtTGS1(201–538)

Repeated attempts to express the full-length AtTGS1 protein in *Escherichia coli* produced only insoluble inclusion bodies, so a construct representing AtTGS1(201–538) was assembled using PCR. The reduced sequence was cloned into vector pLW01-DsRed-His (Roston et al., 2011; Wang et al., 2012) by restriction with *Sac*I and *Not*I, and the sequence of a clone verified. This construct,

fusing DsRed-AtTGS1(201-538)-6×His, was transformed into *E. coli* strain Rosetta(DE3) (Tegel et al., 2010). After dilution of fresh overnight cultures, cells were grown at 37°C, and when OD_{600} of the culture reached 0.7, expression of the protein was induced by addition of 0.2 mM isopropylthio-β-galactoside followed by room temperature incubation overnight. The harvested cells were lysed in CelLytic B buffer (Sigma-Aldrich) and the protein purified by Ni-NTA agarose (Qiagen) according to the manufacturer's protocol. Purified protein samples were dialyzed against buffer (50 mM Tris-HCL, pH 8.0, 200 mM NaCl, 2 mM dithiothreitol, 1 M EDTA, and 10% glycerol) three times for 8 h each at 4°C, then stored at −80°C.

Methyltransferase Assay

Methyltransferase activity of TGS1 was assayed as described (Hausmann et al., 2008) with minor revision. The enzyme reaction mixtures (20 μL) contained 50 mM Tris-HCl, pH 8.0, 5 mM dithiothreitol, 12.5 μM $C^{14}H3$-AdoMet, 5 mM 7-methylguanosine 5′-diphosphate sodium salt (m^7GDP; Sigma-Aldrich), and the proteins as specified. After the mixtures were incubated at 37°C for 1 h, 4 μL aliquots were spotted on PEI-cellulose thin-layer chromatography plates (Sigma-Aldrich) and developed with 50 mM ammonium sulfate for 40 min. The radioactivity in the chromatography plates was detected by exposure to an imaging plate for 4 d, followed by analysis on a Typhoon FLA 7000 (GE Healthcare).

Yeast *tgs1*Δ Complementation

Wild-type and *tgs1*Δ yeast strains were obtained from Dr. Beate Schwer at Weill Cornell Medical College (Hausmann et al., 2008). The AtTGS1 coding sequence was amplified from reverse transcription of RNA purified from wild-type leaves, then cloned into pENTR/D-TOPO (Invitrogen) and the sequence confirmed. The coding sequences of AtTGS1 with mutations D397A and W444A were created by overlap extension PCR (Heckman and Pease, 2007). For deletion of the TGS1 WW domain (amino acids 169–192), a Gibson assembly reaction was used in which *tgs1* was amplified using primers ΔWW-f and ΔWW-r (Supplemental Table S1), and the product was gel purified then assembled using Gibson Assembly Master Mix (New England Biolabs) according to the manufacturer's instructions. These AtTGS1 coding sequence derivatives were cloned into pENTR/D-TOPO, and a sequence-verified clone was transferred to pMK195 (Overvoorde et al., 1996) by the LR-Clonase reaction (Invitrogen). The resulting yeast expression constructs were transformed into yeast *tgs1*Δ and selected on SC-Ura plates. The empty vector was likewise transformed into wild type and *tgs1*Δ to serve as controls. The transformed strains were grown in SC-Ura medium overnight, and the fresh cultures were diluted to OD = 1.0. Indicated dilutions were spotted onto SC-URA plants and the 28°C plate was photographed after 2 d incubation, the 18°C after 8 d.

Phenotypic Analysis of *tgs1* Mutants

The phenotypic examination for normal conditions took place at 22°C after the leaves were dark adapted at room temperature for 30 min. Chlorophyll fluorescence of leaves was measured as previously described (Wu et al., 1997), except the instrument was a Fluorescence Monitoring System FMS1 (Hansatech Instruments). The phenotypic examination under chilling conditions in most instances began with plants geminated and grown at 22°C for 12 d then transferred to 5°C for prolonged growth. In an experiment to specially detect the reproductive phenotypes of *tgs1* mutants, wild-type, *tgs1-1*, and *tgs1-2* lines were grown at 22°C for 45 d in 10 h light conditions before transfer to 5°C for 51 d growth, when they were photographed. To assess plant phenotypes at cool temperatures above 5°C, plants were grown at 22°C for 12 d, then transferred to 10°C for 90 d and photographed. For growth curve analysis, wild type and *tgs1-1* mutants were geminated and grown at 22°C for 10 d, then half the plants were transferred to 5°C growth. The above-soil tissue of three or four random plants was collected and weighed every 5 d from both 22°C and 5°C growth conditions. The raw values were averaged, multiplied by 100 to render the logarithmic graph in positive numbers, and the best fit line determined using GraphPad Prism software. We report the relative growth rate, ω^{-1}, the slope of the natural logarithm of fresh weight over time.

Complementation of *tgs1-1*

To complement the *tgs1-1* mutant, the viral promoter of transformation vector pB7FWG2 (Karimi et al., 2002) was replaced with a 1,298-nucleotide fragment representing the chromosomal DNA just 5′ to the start codon of TGS1, representing the presumptive promoter. The nucleotide sequence comprising the AtTGS1 open reading frame, or the AtTGS1ΔWW derivative, was cloned under the control of this native promoter sequence by the LR-Clonase reaction. After transforming the constructs into *Agrobacterium tumefaciens* GV3101, plants were transformed by floral dip (Clough and Bent, 1998) and transgenic plants detected by Basta resistance. Three *tgs1-1* homozygous plant lines transformed with each construct, which were confirmed as expressing the transgenic construct by RT-PCR analysis, were subjected to growth under chilling conditions and photographed after 35 d at 5°C.

Accession Numbers

Sequence data from this article can be found in the GenBank/EMBL data libraries under accession numbers AEE32102.1, At1g45231, TGS1; AEE31243.2, At1g30550, homologue of TGS1.

Supplemental Data

The following supplemental materials are available.

Supplemental Figure S1. AtTGS1 methyltransferase activity in vitro.

Supplemental Figure S2. Leaf senescence of *tgs1* mutants.

Supplemental Figure S3. Vegetative growth of *tgs1* mutants under different chilling treatments.

Supplemental Figure S4. Expression of AtTGS1 WW domain variants.

Supplemental Table S1. T-DNA mutants with visible phenotypes under 5°C regimen.

Supplemental Table S2. Primers.

ACKNOWLEDGMENTS

We thank Dr. Li Tian of the Institute of Biological Chemistry, Washington State University, for help with protoplast transformation. We also thank Dr. Beate Schwer of the Weill Cornell Medical College for generously providing the *S. cerevisiae tgs1*Δ strain and the human TGS1 expression construct. We thank Dr. Shuangyi Bai for helpful discussions, Dr. Christoph Benning of Michigan State University for providing the pLW01-DsRed-His expression vector, and Dr. Daniel Mullendore at the Franceschi Microscopy and Imaging Center of Washington State University for his help with confocal microscopy.

Received March 8, 2017; accepted May 9, 2017; published May 11, 2017.

LITERATURE CITED

Allen DJ, Ort DR (2001) Impacts of chilling temperatures on photosynthesis in warm-climate plants. Trends Plant Sci **6:** 36–42

Alonso JM, Stepanova AN, Leisse TJ, Kim CJ, Chen H, Shinn P, Stevenson DK, Zimmerman J, Barajas P, Cheuk R, et al (2003) Genome-wide insertional mutagenesis of *Arabidopsis thaliana*. Science **301:** 653–657

Amiard S, Da Ines O, Gallego ME, White CI (2014) Responses to telomere erosion in plants. PLoS One **9:** e86220

Barrero-Gil J, Huertas R, Rambla JL, Granell A, Salinas J (2016) Tomato plants increase their tolerance to low temperature in a chilling acclimation process entailing comprehensive transcriptional and metabolic adjustments. Plant Cell Environ **39:** 2303–2318

Bedford MT, Sarbassova D, Xu J, Leder P, Yaffe MB (2000) A novel pro-Arg motif recognized by WW domains. J Biol Chem **275:** 10359–10369

Boon KL, Pearson MD, Košˇ M (2015) Self-association of Trimethylguanosine Synthase Tgs1 is required for efficient snRNA/snoRNA trimethylation and pre-rRNA processing. Sci Rep **5:** 11282

Brown JW, Echeverria M, Qu LH (2003) Plant snoRNAs: Functional evolution and new modes of gene expression. Trends Plant Sci **8:** 42–49

Brown JW, Shaw PJ, Shaw P, Marshall DF (2005) Arabidopsis nucleolar protein database (AtNoPDB). Nucleic Acids Res **33:** D633–D636

Burroughs AM, Ando Y, Aravind L (2014) New perspectives on the diversification of the RNA interference system: Insights from comparative genomics and small RNA sequencing. Wiley Interdiscip Rev RNA **5:** 141–181

Capovilla G, Pajoro A, Immink RG, Schmid M (2015) Role of alternative pre-mRNA splicing in temperature signaling. Curr Opin Plant Biol **27:** 97–103

Clough SJ, Bent AF (1998) Floral dip: a simplified method for Agrobacterium-mediated transformation of Arabidopsis thaliana. Plant J **16:** 735–743

Edwards K, Johnstone C, Thompson C (1991) A simple and rapid method for the preparation of plant genomic DNA for PCR analysis. Nucleic Acids Res **19:** 1349

Enünlü I, Pápai G, Cserpán I, Udvardy A, Jeang KT, Boros I (2003) Different isoforms of PRIP-interacting protein with methyltransferase domain/trimethylguanosine synthase localizes to the cytoplasm and nucleus. Biochem Biophys Res Commun **309:** 44–51

Filichkin SA, Priest HD, Givan SA, Shen R, Bryant DW, Fox SE, Wong WK, Mockler TC (2010) Genome-wide mapping of alternative splicing in *Arabidopsis thaliana*. Genome Res **20:** 45–58

Foyer CH, Vanacker H, Gomez LD, Harbinson J (2002) Regulation of photosynthesis and antioxidant metabolism in maize leaves at optimal and chilling temperatures: Review. Plant Physiol Biochem **40:** 659–668

Franke J, Gehlen J, Ehrenhofer-Murray AE (2008) Hypermethylation of yeast telomerase RNA by the snRNA and snoRNA methyltransferase Tgs1. J Cell Sci **121:** 3553–3560

Gao J, Wallis JG, Browse J (2015) Mutations in the prokaryotic pathway rescue the fatty acid biosynthesis1 mutant in the cold. Plant Physiol **169:** 442–452

Ghosh A, Lima CD (2010) Enzymology of RNA cap synthesis. Wiley Interdiscip Rev RNA **1:** 152–172

Guan YJ, Hu J, Wang XJ, Shao CX (2009) Seed priming with chitosan improves maize germination and seedling growth in relation to physiological changes under low temperature stress. J Zhejiang Univ Sci B **10:** 427–433

Hausmann S, Shuman S (2005) Specificity and mechanism of RNA cap guanine-N2 methyltransferase (Tgs1). J Biol Chem **280:** 4021–4024

Hausmann S, Zheng S, Costanzo M, Brost RL, Garcin D, Boone C, Shuman S, Schwer B (2008) Genetic and biochemical analysis of yeast and human cap trimethylguanosine synthase: Functional overlap of 2,2,7-trimethylguanosine caps, small nuclear ribonucleoprotein components, pre-mRNA splicing factors, and RNA decay pathways. J Biol Chem **283:** 31706–31718

Heckman KL, Pease LR (2007) Gene splicing and mutagenesis by PCR-driven overlap extension. Nat Protoc **2:** 924–932

Holdsworth MJ, Bentsink L, Soppe WJ (2008) Molecular networks regulating Arabidopsis seed maturation, after-ripening, dormancy and germination. New Phytol **179:** 33–54

Iida K, Seki M, Sakurai T, Satou M, Akiyama K, Toyoda T, Konagaya A, Shinozaki K (2004) Genome-wide analysis of alternative pre-mRNA splicing in *Arabidopsis thaliana* based on full-length cDNA sequences. Nucleic Acids Res **32:** 5096–5103

Jia Y, Viswakarma N, Crawford SE, Sarkar J, Sambasiva Rao M, Karpus WJ, Kanwar YS, Zhu YJ, Reddy JK (2012) Early embryonic lethality of mice with disrupted transcription cofactor PIMT/NCOA6IP/Tgs1 gene. Mech Dev **129:** 193–207

Jiao Y, Meyerowitz EM (2010) Cell-type specific analysis of translating RNAs in developing flowers reveals new levels of control. Mol Syst Biol **6:** 419

Karimi M, Inzé D, Depicker A (2002) GATEWAY vectors for Agrobacterium-mediated plant transformation. Trends Plant Sci **7:** 193–195

Knight MR, Knight H (2012) Low-temperature perception leading to gene expression and cold tolerance in higher plants. New Phytol **195:** 737–751

Komonyi O, Pápai G, Enunlu I, Muratoglu S, Pankotai T, Kopitova D, Maróy P, Udvardy A, Boros I (2005) DTL, the *Drosophila* homolog of PIMT/Tgs1 nuclear receptor coactivator-interacting protein/RNA methyltransferase, has an essential role in development. J Biol Chem **280:** 12397–12404

Kupsch C, Ruwe H, Gusewski S, Tillich M, Small I, Schmitz-Linneweber C (2012) Arabidopsis chloroplast RNA binding proteins CP31A and CP29A associate with large transcript pools and confer cold stress tolerance by influencing multiple chloroplast RNA processing steps. Plant Cell **24:** 4266–4280

Lazar G, Goodman HM (2000) The Arabidopsis splicing factor SR1 is regulated by alternative splicing. Plant Mol Biol **42:** 571–581

Levitt J (1980) Responses of Plants to Environmental Stresses. **Vol 2:** Water, Radiation, Salt, and Other Stresses. Academic Press, Cambridge, MA

Lin W, Block G (2009) Chilling injury of sweet potato shoots reduced by prior incubation of H2O2 and NaCl. Open Horticulture Journal **2:** 1–5

Lukatkin AS, Brazaityte A, Bobinas C, Duchovskis P (2012) Chilling injury in chilling-sensitive plants: A review. Zemdirbyste **99:** 111–124

Lv Y, Guo Z, Li X, Ye H, Li X, Xiong L (2016) New insights into the genetic basis of natural chilling and cold shock tolerance in rice by genome-wide association analysis. Plant Cell Environ **39:** 556–570

Lyons JM (1973) Chilling injury in plants. Annu Rev Plant Physiol **24:** 445–466

Ma Y, Dai X, Xu Y, Luo W, Zheng X, Zeng D, Pan Y, Lin X, Liu H, Zhang D, et al (2015) COLD1 confers chilling tolerance in rice. Cell **160:** 1209–1221

Macias MJ, Wiesner S, Sudol M (2002) WW and SH3 domains, two different scaffolds to recognize proline-rich ligands. FEBS Lett **513:** 30–37

Meyer K, Koester T, Staiger D (2015) Pre-mRNA Splicing in Plants: In Vivo Functions of RNA-Binding Proteins Implicated in the Splicing Process. Biomolecules **5:** 1717–1740

Miao Y, Jiang L (2007) Transient expression of fluorescent fusion proteins in protoplasts of suspension cultured cells. Nat Protoc **2:** 2348–2353

Miura K, Furumoto T (2013) Cold signaling and cold response in plants. Int J Mol Sci **14:** 5312–5337

Monecke T, Dickmanns A, Ficner R (2009) Structural basis for m7G-cap hypermethylation of small nuclear, small nucleolar and telomerase RNA by the dimethyltransferase TGS1. Nucleic Acids Res **37:** 3865–3877

Mouaikel J, Bujnicki JM, Tazi J, Bordonné R (2003) Sequence-structure-function relationships of Tgs1, the yeast snRNA/snoRNA cap hypermethylase. Nucleic Acids Res **31:** 4899–4909

Mouaikel J, Verheggen C, Bertrand E, Tazi J, Bordonné R (2002) Hypermethylation of the cap structure of both yeast snRNAs and snoRNAs requires a conserved methyltransferase that is localized to the nucleolus. Mol Cell **9:** 891–901

Otte L, Wiedemann U, Schlegel B, Pires JR, Beyermann M, Schmieder P, Krause G, Volkmer-Engert R, Schneider-Mergener J, Oschkinat H (2003) WW domain sequence activity relationships identified using ligand recognition propensities of 42 WW domains. Protein Sci **12:** 491–500

Overvoorde PJ, Frommer WB, Grimes HD (1996) A soybean sucrose binding protein independently mediates nonsaturable sucrose uptake in yeast. Plant Cell **8:** 271–280

Patterson BD, Reid MS (1990) Genetic and environmental influences on the expression of chilling injury. *In* CY Wang, ed, Chilling Injury of Horticultural Crops. CRC Press, Boca Raton, FL, pp 87–112

Paull RE (1990) Chilling injury of crops of tropical and subtropical origin. *In* CY Wang, ed, Chilling Injury of Horticultural Crops. CRC Press, Boca Raton, FL, pp 17–36

Pendle AF, Clark GP, Boon R, Lewandowska D, Lam YW, Andersen J, Mann M, Lamond AI, Brown JW, Shaw PJ (2005) Proteomic analysis of the Arabidopsis nucleolus suggests novel nucleolar functions. Mol Biol Cell **16:** 260–269

Penfield S, Springthorpe V (2012) Understanding chilling responses in Arabidopsis seeds and their contribution to life history. Philos Trans R Soc Lond B Biol Sci **367:** 291–297

Palusa SG, Ali GS, Reddy AS (2007) Alternative splicing of pre-mRNAs of Arabidopsis serine/arginine-rich proteins: regulation by hormones and stresses. Plant J **49:** 1091–1107

Porat R, Guy CL (2007) Arabidopsis as a model system to study chilling tolerance mechanisms in plants. Plant Stress **1:** 85–92

Provart NJ, Alonso J, Assmann SM, Bergmann D, Brady SM, Brkljacic J, Browse J, Chapple C, Colot V, Cutler S, et al (2016) 50 years of Arabidopsis research: Highlights and future directions. New Phytol **209:** 921–944

Qiu ZR, Chico L, Chang J, Shuman S, Schwer B (2012) Genetic interactions of hypomorphic mutations in the m7G cap-binding pocket of yeast nuclear cap binding complex: An essential role for Cbc2 in meiosis via splicing of MER3 pre-mRNA. RNA **18:** 1996–2011

Qiu ZR, Schwer B, Shuman S (2015) Two routes to genetic suppression of RNA trimethylguanosine cap deficiency via C-terminal truncation of U1 snRNP subunit Snp1 or overexpression of RNA polymerase subunit Rpo26. G3 (Bethesda) **5:** 1361–1370

Qiu ZR, Shuman S, Schwer B (2011) An essential role for trimethylguanosine RNA caps in *Saccharomyces cerevisiae* meiosis and their requirement for splicing of SAE3 and PCH2 meiotic pre-mRNAs. Nucleic Acids Res **39:** 5633–5646

Riha K, McKnight TD, Griffing LR, Shippen DE (2001) Living with genome instability: Plant responses to telomere dysfunction. Science **291:** 1797–1800

Roston R, Gao J, Xu C, Benning C (2011) Arabidopsis chloroplast lipid transport protein TGD2 disrupts membranes and is part of a large complex. Plant J **66:** 759–769

Schneider JC, Hugly S, Somerville CR (1995) Chilling-sensitive mutants of Arabidopsis. Plant Mol Biol Rep **13:** 11–17

Schwacke R, Fischer K, Ketelsen B, Krupinska K, Krause K (2007) Comparative survey of plastid and mitochondrial targeting properties of transcription factors in Arabidopsis and rice. Mol Genet Genomics **277:** 631–646

Shimba S, Buckley B, Reddy R, Kiss T, Filipowicz W (1992) Cap structure of U3 small nucleolar RNA in animal and plant cells is different. gamma-Monomethyl phosphate cap structure in plant RNA. J Biol Chem **267:** 13772–13777

Siena LA, Ortiz JP, Leblanc O, Pessino S (2014) PnTgs1-like expression during reproductive development supports a role for RNA methyltransferases in the aposporous pathway. BMC Plant Biol **14:** 297

Streitner C, Simpson CG, Shaw P, Danisman S, Brown JW, Staiger D (2013) Small changes in ambient temperature affect alternative splicing in Arabidopsis thaliana. Plant Signal Behav **8:** e24638

Swaraz AM, Park YD, Hur Y (2011) Knock-out mutations of Arabidopsis SmD3-b induce pleotropic phenotypes through altered transcript splicing. Plant Sci **180:** 661–671

Tang W, Kannan R, Blanchette M, Baumann P (2012) Telomerase RNA biogenesis involves sequential binding by Sm and Lsm complexes. Nature **484:** 260–264

Tegel H, Tourle S, Ottosson J, Persson A (2010) Increased levels of recombinant human proteins with the *Escherichia coli* strain Rosetta(DE3). Protein Expr Purif **69:** 159–167

Thakur P, Kumar S, Malik JA, Berger JD, Nayyar H (2010) Cold stress effects on reproductive development in grain crops: An overview. Environ Exp Bot **67:** 429–443

Thomashow MF (1999) Plant cold acclimation: Freezing tolerance genes and regulatory mechanisms. Annu Rev Plant Physiol Plant Mol Biol **50:** 571–599

Thomashow MF (2010) Molecular basis of plant cold acclimation: Insights gained from studying the CBF cold response pathway. Plant Physiol **154:** 571–577

Tokuhisa J (1999) Genetic engineering of plant chilling tolerance. *In* JK Setlow, ed, Genetic Engineering, **Vol 21**. Springer, New York, pp 79–93

Tokuhisa JG, Feldmann KA, LaBrie ST, Browse J (1997) Mutational analysis of chilling tolerance in plants. Plant Cell Environ **20:** 1391–1400

Tokuhisa JG, Vijayan P, Feldmann KA, Browse JA (1998) Chloroplast development at low temperatures requires a homolog of DIM1, a yeast gene encoding the 18S rRNA dimethylase. Plant Cell **10:** 699–711

Truernit E, Bauby H, Dubreucq B, Grandjean O, Runions J, Barthélémy J, Palauqui JC (2008) High-resolution whole-mount imaging of three-dimensional tissue organization and gene expression enables the study of Phloem development and structure in Arabidopsis. Plant Cell **20:** 1494–1503

Usadel B, Bläsing OE, Gibon Y, Poree F, Höhne M, Günter M, Trethewey R, Kamlage B, Poorter H, Stitt M (2008) Multilevel genomic analysis of the response of transcripts, enzyme activities and metabolites in Arabidopsis rosettes to a progressive decrease of temperature in the non-freezing range. Plant Cell Environ **31:** 518–547

Vallejos CE, Pearcy RW (1987) Differential acclimation potential to low temperatures in two species of Lycopersicon: Photosynthesis and growth. Can J Bot **65:** 1303–1307

Vinocur B, Altman A (2005) Recent advances in engineering plant tolerance to abiotic stress: Achievements and limitations. Curr Opin Biotechnol **16:** 123–132

Wang CY (1990) Chilling Injury of Horticultural Crops. CRC Press, Boca Raton, FL

Wang S, Bai G, Wang S, Yang L, Yang F, Wang Y, Zhu JK, Hua J (2016) Chloroplast RNA-binding protein RBD1 promotes chilling tolerance through 23S rRNA processing in Arabidopsis. PLoS Genet **12:** e1006027

Wang Z, Xu C, Benning C (2012) TGD4 involved in endoplasmic reticulum-to-chloroplast lipid trafficking is a phosphatidic acid binding protein. Plant J **70:** 614–623

Wang H, You C, Chang F, Wang Y, Wang L, Qi J, Ma H (2014) Alternative splicing during Arabidopsis flower development results in constitutive and stage-regulated isoforms. Front Genet **5:** 25

Wu J, Lightner J, Warwick N, Browse J (1997) Low-temperature damage and subsequent recovery of fab1 mutant Arabidopsis exposed to 2 degrees C. Plant Physiol **113:** 347–356

Zhu Y, Qi C, Cao WQ, Yeldandi AV, Rao MS, Reddy JK (2001) Cloning and characterization of PIMT, a protein with a methyltransferase domain, which interacts with and enhances nuclear receptor coactivator PRIP function. Proc Natl Acad Sci USA **98:** 10380–10385

Zinn KE, Tunc-Ozdemir M, Harper JF (2010) Temperature stress and plant sexual reproduction: Uncovering the weakest links. J Exp Bot **61:** 1959–1968

Zipperlen P, Fraser AG, Kamath RS, Martinez-Campos M, Ahringer J (2001) Roles for 147 embryonic lethal genes on *C. elegans* chromosome I identified by RNA interference and video microscopy. EMBO J **20:** 3984–3992